Journal of Alloys and Compounds 819 (2020) 153052

Contents lists available at ScienceDirect

Journal of Alloys and Compounds

journal homepage: http://www.elsevier.com/locate/jalcom

Impact of annealing temperature on band-alignment of PLD grown Ga_2O_3/Si (100) heterointerface

Manoj K. Yadav, Arnab Mondal, Subhashis Das, Satinder K. Sharma, Ankush Bag*

School of Computing and Electrical Engineering, Indian Institute of Technology Mandi, Himachal Pradesh, 175005, India

ARTICLE INFO

Article history:
Received 10 August 2019
Received in revised form
25 October 2019
Accepted 15 November 2019
Available online 16 November 2019

Keywords:
β-Ga_2O_3
Annealing
Band alignment
XPS
Silicon (100)
Pulsed laser deposition

ABSTRACT

Cost-effective integration with existing silicon CMOS electronics has been one of the primary motivations for most of the emerging non-silicon devices. In this context, β-gallium oxide (Ga_2O_3) films were deposited on Si (100) substrate using pulsed laser deposition (PLD) technique in this research. After deposition, samples were further annealed at 600 °C and 800 °C under vacuum. X-ray diffractometer (XRD) was employed to observe the crystallinity variation due to the annealing. The crystallinity of samples degrades with annealing at 600 °C and an incremental improvement in crystallinity was again exhibited at 800 °C due to the possible rearrangement of the Ga and O atoms to their optimal sites. Further, x-ray photoelectron spectroscopy (XPS) was used for identification of elements and chemical composition. XPS results were also analyzed to locate the position of Ga 2p and Si 2p core levels and calculate the valance band offset (VBO) at Ga_2O_3/Si interface. Reflected electron energy loss spectroscopy (REELS) and ultraviolet photoelectron spectroscopy (UPS) were utilized to calculate the bandgap and work function, respectively. Moreover, valance band maxima and Fermi level position of the as-deposited and annealed samples were calculated using UPS. The bandgaps for the as-deposited, annealed samples at 600 °C and 800 °C were estimated to be 4.72 ± 0.05, 4.52 ± 0.05, and 4.48 ± 0.05 eV, respectively. Consequently, the work function of the sample increases with annealing due to increase in the oxygen vacancies and resulting bandgap narrowing. The band offsets (valance band, conduction band) were determined to be (3.35 ± 0.05 eV, 0.26 ± 0.02 eV), (3.55 ± 0.05 eV, 0.15 ± 0.02 eV) and (3.54 ± 0.05 eV, 0.17 ± 0.02 eV) for the as-deposited, annealed samples at 600 °C and 800 °C, respectively. This optimization of band alignment with annealing temperature shall be very useful for controlling the carrier transport at the interface for Ga_2O_3/Si based devices. Thus, a trade-off is to be performed between VBO and crystallinity of the Ga_2O_3/Si to operate the devices efficiently and reliably respectively.

© 2019 Elsevier B.V. All rights reserved.

1. Introduction

β-Ga_2O_3 is a wide bandgap semiconductor with a varying bandgap of 4.4–4.9 eV [1–3]. There are five different phases of Ga_2O_3, however, monoclinic (β) polymorph is the most stable and widely used for device applications [4–6]. Owing to such an ultra-wide bandgap, β-Ga_2O_3 has very high breakdown electric field (8 MV/cm), thus it acts as a promising candidate for next-generation high power electronic devices [7,8]. This material can also be used for UV optoelectronic devices due to high-transparency in the visible range [2,9,10]. The thermal stability of the material is also excellent which leads to applications for high-temperature oxygen gas sensors [11–13]. Additionally, Ga_2O_3 heterojunctions with Al_2O_3, GaN, SiC, ZnO and Si substrates have been investigated for numerous applications such as photodetectors [14–21], light-emitting diodes (LEDs) [22,23], and power switching devices [24–26]. Heterojunction between Ga_2O_3 and Si [27] is relatively more attractive because of the several inherent and well-known properties of Si substrate, such as high stability, low cost, and abundance on the earth, and its wide applications in the integrated CMOS circuits. An additional advantage of Ga_2O_3 integration with Si for high power devices is the efficient dissipation of heat due to the higher thermal conductivity of Si (150 $Wm^{-1}K^{-1}$) than the Ga_2O_3 (8.8 ± 3.4 $Wm^{-1}K^{-1}$). It is known that the bandgap of any semiconductor is an inherent material property and annealing can decrease it to some extent [28,29]. The semiconductor work function which is an energy gap between the Fermi level to the vacuum level also depends on the mentioned

* Corresponding author.
E-mail address: bag.ankush@gmail.com (A. Bag).

https://doi.org/10.1016/j.jallcom.2019.153052
0925-8388/© 2019 Elsevier B.V. All rights reserved.

temperature. When we change the annealing temperature, there will be a shift in the Fermi level, and the consequent changes in the work function. As unintentionally doped Ga_2O_3 is an n-type semiconductor [30], if we increase the annealing temperature, the work function will also increase. It is well known that the band offset is one of the most critical electronic parameters in deciding the carrier transport nature in the semiconductor heterojunction [27]. Band offset provides the energy barriers height experienced by the charge carriers to cross a junction. Chen et al. [27] have found the VBO of Ga_2O_3/Si (111) heterojunction to be 3.5 eV using XPS. However, Si (100) is the most preferred orientation for the actual integration of emerging electronics with existing CMOS technology. Though several studies have been conducted for the deposition of Ga_2O_3 on Si (100), the band alignment and its effect on post-annealing temperature on the Ga_2O_3/Si (100) have not been investigated yet. In this work, XPS is used to investigate the electronic interface structure and band alignment of Ga_2O_3/Si (100) heterojunctions. The band offset values are calculated for as-deposited and annealed at 600 °C and 800 °C samples. The Ga_2O_3/Si heterojunction is observed as a type-I heterojunction. Further, it has been seen that band alignment is varying with annealing temperature and will be helpful to improve the performance of the devices.

2. Experimental details

Ga_2O_3 powder (purity 99.999%) was purchased from Sigma Aldrich Company (USA). The Ga_2O_3 pellet was made from the powder and placed inside the furnace at a sintering temperature of 1200 °C for 24 h. P-type Si (100) wafer has been cleaned by Radio Corporation of America (RCA) process (SC-1 and SC-2) of wafer cleaning. Then, the Si wafer was cleaned with Hydrogen Fluoride (HF) acid to remove additional native oxide layers.

Ga_2O_3 thin film was deposited on Si (100) substrate using a cluster tool-based pulsed laser deposition (PLD) from PREVAC, Poland. The base pressure of the deposition chamber was 5×10^{-8} Torr, and the substrate was heated at 635 °C temperature. The β- Ga_2O_3 thin films were deposited under an O_2 atmosphere for 35 min. The processing pressure was 1.3×10^{-3} Torr, the O_2 flow rate was 8.1 sccm. The repetition rate and laser energy were fixed at 5 Hz and 200 mJ/cm^2, respectively. The thickness of the thin film was 110 nm as confirmed by the ellipsometer instrument. To investigate the effect of annealing, the film deposited at a substrate temperature of 635 °C was cut into three pieces. Two samples were placed inside a tube furnace. Samples were further annealed at two different temperatures of 600 °C and 800 °C for 1 h under a vacuum of 5×10^{-3} mbar. We have strategically selected these two annealing temperatures in order to understand the annealing effect on the Ga_2O_3 and its hetero-junction with p-Si (100). Thereby, one temperature has been kept above sample growth temperature (635 °C) and another one is below 635 °C. If we anneal the sample at temperatures far below than the growth temperature, there is no expected effect of annealing on the crystalline quality of the film.

Furthermore, if we anneal the sample beyond 800 °C, the crystalline quality of the film might decrease drastically. Therefore, we have chosen to anneal the samples around the growth temperature for a longer duration. Moreover, the range of 600 °C–800 °C has been found to be the optimized temperature for annealing of the Ga_2O_3 thin films in previously reported literature also [31,32]. Hence, we believe that these two temperatures are sufficient to study the effect of annealing on the samples in present context. Additionally, while most of the reports are showing an annealing effect on the crystalline quality, oxygen vacancies, and the roughness of the Ga_2O_3 films [33,34]. We are showing the effect of annealing on band alignment parameters of n-Ga_2O_3/p-Si (100) hetero-junction, which has been not yet reported.

The crystalline quality of the Ga_2O_3 samples was examined by an X-ray diffractometer (Smart lab, Rigaku Japan; XRD) with a scan range of 20°–80°. Cu K_α was used as the X-ray source with the wavelength of λ=0.154 nm. XPS survey scan was used to identify the elements present on the thin film and to determine the chemical state of the elements. Thermo scientific NEXSA XPS with Al K_α X-ray source with the energy of 1486 eV was used. The angle between analyzer and sample surface was 90°, analysis size of 400 μm diameter, with source power of 72 W, pass energy for survey scans of 200 eV, and pass energy for high-resolution scans of 50 eV. The electron gun was used to perform charge compensation. Further, to nullify the effect of peak shift due to charge accumulation in the non-conducting sample, the adventitious carbon line in C 1s spectra at 284.8 eV was used.

Reflection electron energy loss spectroscopy (REELS) with a pass energy of 5 eV was used to obtain the bandgap of the Ga_2O_3 thin films and Si substrate. Ultra-violet photoelectron spectroscopy (UPS) with a pass energy of 1 eV, a target current of 50 mA was used to calculate the work function of the materials. Here, He I e (21 eV) was used to turn on the UV source.

3. Results and discussion

To investigate the effect of annealing on the crystallinity of β-Ga_2O_3 films deposited on Si (100) substrates, the XRD study was done on as-deposited and annealed at 600 °C and 800 °C samples. Fig. 1(a) shows the XRD diffraction patterns of the β-Ga_2O_3 films. All three samples show the polycrystalline β-Ga_2O_3 with monoclinic structure. Ga_2O_3 material shows polymorphism. Phase- β is the only stable polymorphs throughout the whole temperature range until its melting point (1900 °C). XRD pattern of as-deposited samples shows polycrystalline nature of β-Ga_2O_3, however the high-temperature annealing for a long time might degrade the crystal quality of the films as reported by Feng et al. [32]. This degradation has also been confirmed in our observations. It can be clearly observed that the crystalline quality is better for as-deposited Ga_2O_3 sample than the annealed samples. The (−201) peak is dominant for as-deposited sample, while for the samples annealed at 600 °C and 800 °C the (−201) peak vanishes, leading the annealed samples towards poor crystal quality. Again, the intensity at (−401) plane degrades for sample annealed at 600 °C than as-deposited sample, while a little bit of improvement is observed for the sample annealed at 800 °C as compared to the sample annealed at 600 °C. In case of sample annealed at 600 °C, annealing temperature is lowered than that of the growth temperature, and the vacuum environment during annealing might have reduced the crystallinity in presence of more vacancy. However, a little improvement in crystallinity was again exhibited at 800 °C annealing due to the possible rearrangement of the Ga and O atoms at their optimal sites.

The other parameters full width at half maximum (FWHM) and crystallite size of the samples are also calculated from the XRD patterns listed in Table 1. The FWHM is observed from the (−401) peak of the XRD pattern, and the crystallite size is calculated using the Scherrer's equation. The FWHM value is increasing while the sample is being annealed as compared to as-deposited samples. However, FWHM decreases for sample annealed at 800 °C as compared to the sample annealed at 600 °C. The FWHM values are 0.5009°, 0.5054°, and 0.5032° for as-deposited Ga_2O_3, samples annealed at 600 °C, and 800 °C respectively. The crystal quality of the Ga_2O_3 is reducing because FWHM values are increasing, and the crystallite size is decreasing for the annealed samples.

The XPS survey scan of as-grown Ga_2O_3 thin film and defect-free silicon substrate has been shown in Fig. 2 (a). The Ga_2O_3 thin film

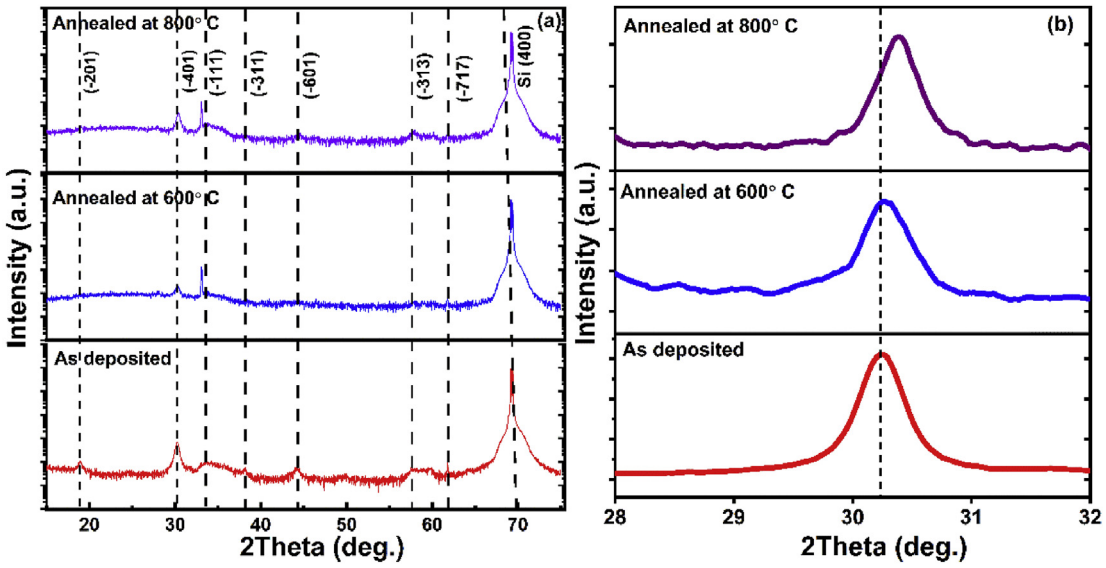

Fig. 1. (a) XRD pattern of as-deposited, annealed at 600 °C and 800 °C thin films (b) Peak shift in the XRD pattern of annealed samples.

Table 1
Parameters observed from the XRD pattern of the samples.

Sample Name	FWHM(degree)	Crystallite Size (nm)
Ga_2O_3 as-deposited	0.5009	16.47
Ga_2O_3 annealed at 600 °C	0.5050	16.33
Ga_2O_3 annealed at 800 °C	0.5032	16.40

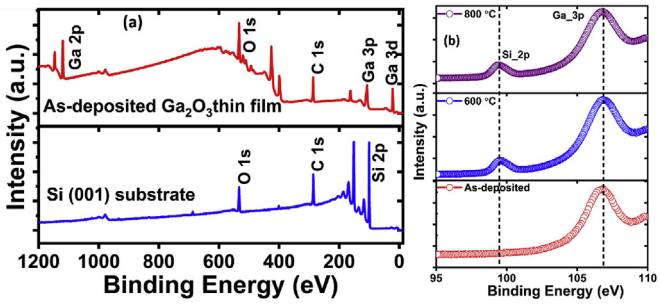

Fig. 2. XPS survey spectra of Ga_2O_3 as-grown thin film and Si (100) substrate (b) showing Si diffusion for annealed samples.

survey spectra show the characteristic peaks of Ga (2p, 3p, 3d), O 1s, and C 1s, whereas the spectra for Si shows Si 2p, O 1s, and C 1s peaks. In the XPS survey spectra of Ga_2O_3 thin films, there is no peak of Si substrate. Thus, from this survey scans, it has been cleared that the Si substrate is not transferred to the thin film surface. The carbon peak (C 1s) has been observed in the survey spectra of both results from the contamination due to exposure in the atmosphere. The O 1s peak in Si survey scan is attributed due to the thin oxide layer formed on the Si substrate.

Si is not transferred from the substrate to the Ga_2O_3 film in the case of the as-deposited sample. However, when the samples are annealed at different temperatures, there is diffusion of Si from the substrate as shown in Fig. 2(b). Henkel et al. [35] have observed that when the sample annealed at higher temperature Si diffused into Oxide from the Si substrate. Fleischer et al. [36] and Battiston et al. [37] also investigated that there is a diffusion of Al in the Ga_2O_3 film from the Al_2O_3 substrate while the sample annealed at higher temperatures. Liu et al. [38] reported that Si is diffused into the GaN at high annealing temperatures.

The stacked XPS narrow scans of thin (110 nm) Ga_2O_3 films on Si (100) substrate at different annealing temperatures for Ga 3d level, Ga 2p core level, and O 1s level are shown in Fig. 3(a), 3(b) and 3(c), respectively. There is a shift in binding energy (BE) with different annealing temperatures. There were no contaminations of metals in the thin films within the measuring limit of XPS, so that the bandgap will not be altered by contaminations, and will not affect the band offsets. From Fig. 3 (a), we detect that the BE of Ga 3d appears at 20.54 eV, and shifted by a BE of 0.17 eV with an increase in annealing temperature. Since the samples were annealed under the vacuum environment, there is a decrement of oxygen atoms, as evident from the compositional ratio of Ga and O. Ga and O composition ratio were 0.72, 0.85, and 0.86 for as-deposited, sample annealed at 600 °C, and 800 °C respectively measured using XPS. This scarcity of oxygen atoms leads to increament of the oxygen vacancies, thereby, the free carrier concentration is also increased. Thus, there is a shift in the Fermi level in the case of the samples annealed at higher temperatures. Fermi level movement exactly matches with variation of VBM (valance band maximum) values with annealing temperatures, are listed in Table 3. Therefore, there is shift in the binding energy because of the Fermi level movement. Kumar et al. [39] have observed that with the higher annealing temperature the binding energy peaks were shifted to the higher binding energy is found because of Fermi level movement, and the shift in the Fermi level is observed by VBM values which exactly matches with variation of VBM values. We also overserved that the shifting of BE for Ga 2p and O 1s spectra are the same as Ga 3d spectra at the different annealing temperatures.

Additionally, as the samples were annealed under the vacuum environment, there is a decrement of oxygen atoms evident from the compositional ratio of Ga and O_2. The Ga and O composition ratio were 0.72, 0.85, and 0.86 for as-deposited, sample annealed at 600 °C, and 800 °C respectively as measured using XPS. This scarcity of oxygen atoms will increase the more oxygen vacancies in the crystal leading to more defects [1]. The peak shift (shown in Fig. 1(b)) in the XRD pattern of annealed films may be correlated to this possible compositional differences as a result of annealing [31,40]. There are different compositions of Ga and O for all three samples. Thus, there are shifting in the peaks of annealed samples.

The stoichiometric ratio between Ga and O is improving with

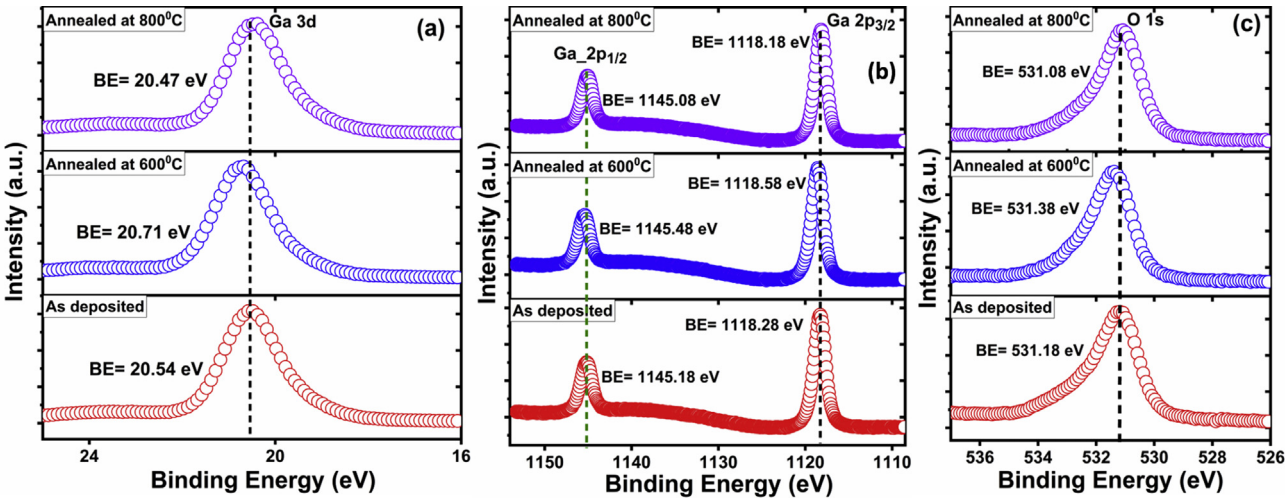

Fig. 3. (a) Stacked XPS narrow spectra of Ga 3d levels. (b) XPS narrow spectra of Ga 2p core levels. (c) XPS naerrow spectra of O 1s levels.

higher annealing temperature due to the desorption of interstitial oxygen atoms. The bandgap of the different samples has been determined using the REELS technique. The bandgap calculation for as-deposited Ga_2O_3 thin film is shown in Fig. 4 (a). The values of the bandgap for as-grown and annealed samples at a different temperature along with Si substrate are listed in Table 2. The calculated value of bandgap for the Si substrate is 1.12 ± 0.01 eV at room temperature. From Table 2, it can be seen that the bandgap decreases as annealing temperature rises.

UPS technique has been used to measure the work function of the different samples. The work function calculation for as-deposited Ga_2O_3 thin film is shown in Fig. 4 (b). From Fig. 4(b), the cut-off BE of Ga_2O_3 is 5.24 eV, Fermi level kinetic energy (KE) is 20.0 eV, and the total photon energy of the system is 21.22 eV. Using these energy values, the work function for the as-deposited Ga_2O_3 sample has been found out to be 5.556 ± 0.1 eV. The work function of all the samples is also listed in Table 2. Since samples were annealed under the vacuum environment, there is decrement of oxygen atoms. This scarcity of oxygen atoms increases the oxygen vacancies. It has been observed that the annealing will cause the diffusion of Si [36,37,41]. Si atoms from the substrate will diffuse into Ga_2O_3 film during annealing of the sample and potentially fill those vacancies. With the higher annealing temperature, the oxygen vacancies will increase leading to more interstitial defects [42–44]. Discrete energy levels due to these defects alongwith filled Si atoms near the conduction band might lead to formation of a band with increament of number of defects. This phenomena will cause to downward the bottom of the conduction band energy. Thereby, when the annealing temperature will increase, conduction band of Ga_2O_3 will also decrease which further leads to decreament of bandgap. Thus, diffused Si atoms in the Ga_2O_3 film will enhance the electron affinity of the Ga_2O_3 film. Therefore, the work function decreases with increase in annealing temperature due to the change in the electron affinity. Furthermore, the bandgap narrowing due to the annealing leads to increment of work-function. This phenomena has already been reported by Kobayashi et al. [45].

Table 2
Calculated values of bandgap and work function for different samples.

Sample	Bandgap (eV)	Work function (eV)
Si (100)	1.12 ± 0.1	4.72 ± 0.1
Ga_2O_3 as deposited	4.72 ± 0.1	5.55 ± 0.1
Ga_2O_3 annealed at 600 °C	4.52 ± 0.1	5.77 ± 0.1
Ga_2O_3 annealed at 800 °C	4.48 ± 0.1	5.77 ± 0.1

Valance band maximum (VBM) of samples can be determined using the UPS spectrum. Fig. 5(a) shows the VBM calculation of the as-deposited Ga_2O_3 sample. The BE values at which the VBM occurs for all the samples are listed in Table 3. The core-level XPS spectrum

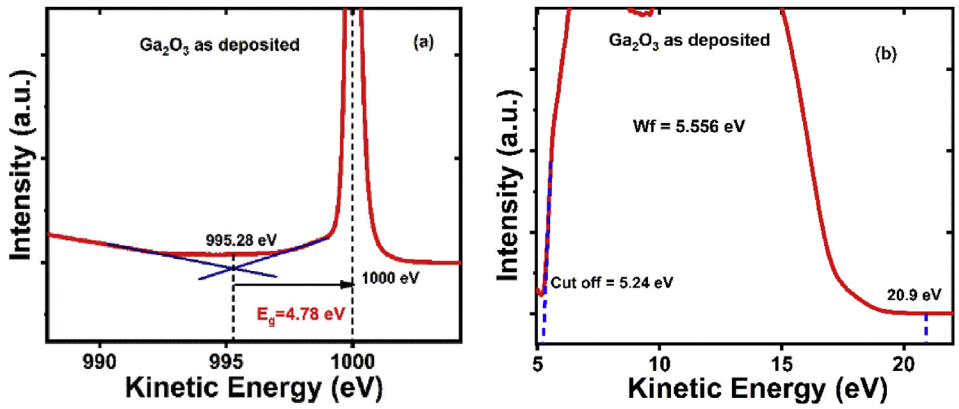

Fig. 4. Calculation of (a) band gap and (b) work function for Ga_2O_3 as-deposited sample using REELS and UPS respectively.

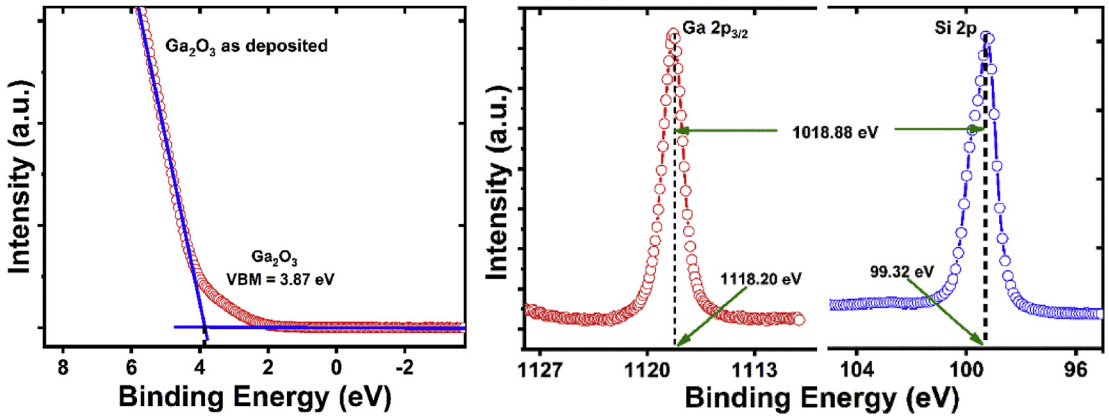

Fig. 5. (a). VBM calculation for as-deposited Ga_2O_3 sample. (b) High resolution XPS spectra for Ga_2O_3 to Si core-core levels.

Table 3
The binding energy of core levels and VBM.

Sample	State	Binding Energy (eV)
Ga_2O_3 as deposited	$E^{Ga_2O_3}_{Ga\_2p}$	1118.20 ± 0.05
Ga_2O_3 as deposited	$E^{Ga_2O_3}_{V}$	3.87 ± 0.1
Ga_2O_3 annealed at 600 °C	$E^{Ga_2O_3}_{Ga\_2p}$	1118.20 ± 0.05
Ga_2O_3 annealed at 600 °C	$E^{Ga_2O_3}_{V}$	4.043 ± 0.1
Ga_2O_3 annealed at 800 °C	$E^{Ga_2O_3}_{Ga\_2p}$	1118.20 ± 0.05
Ga_2O_3 annealed at 800 °C	$E^{Ga_2O_3}_{V}$	4.032 ± 0.1
Si (100)	$E^{Si}_{Si\_2p}$	99.32 ± 0.2
Si (100)	E^{Si}_{V}	0.495 ± 0.1

of Ga_2O_3 and Si substrate has been used to determine the band alignment of Ga_2O_3 and Si heterojunction. Narrow scan XPS spectra have been used to determine the core levels of the samples. Fig. 5(b) shows the BE of the Ga 2p and Si 2p core levels, and core to core level BE the difference. The core level BE for the as-deposited Ga_2O_3 thin film, and Si substrate are to be 1118.20 ± 0.05 eV and 99.32 ± 0.2 eV, respectively. VBM and core level XPS spectra of the thin films and the substrate were used to calculate the valence band offset (VBO) and conduction band offset (CBO).

The VBO (ΔE_V) of the Ga_2O_3/Si (100) has been calculated using Kraut's method [27,46,47] as follow:

$$\Delta E_V = \left(E^{Si}_V - E^{Si}_{Si\_2p}\right) - \left(E^{Ga_2O_3}_V - E^{Ga_2O_3}_{Ga\_2p_{3/2}}\right) + \Delta E_{CL} \quad (1)$$

$$\Delta E_{CL} = \left(E^{Si}_{Si\_2p} - E^{Ga_2O_3}_{Ga\_2p_{3/2}}\right) \quad (2)$$

where E^{Si}_V is the BE of VBM for the substrate, $E^{Ga_2O_3}_V$ is the BE of VBM for Ga_2O_3 thin films, and ΔE_{CL} is core to core level BE energy difference between Si and Ga_2O_3 samples.

Now, the conduction band offset (CBO) can be calculated as

$$\Delta E_C = E^{Ga_2O_3}_g - \left(\Delta E_V + E^{Si}_g\right) \quad (3)$$

where ΔE_C is the conduction band offset, $E^{Ga_2O_3}_g$ is the bandgap of Ga_2O_3 thin films, and E^{Si}_g is bandgap of Si substrate at room temperature. The measured values of the bandgap for all samples are listed in Table 2.

The general schematic band alignment diagram for Ga_2O_3/Si heterojunction is shown in Fig. 6(a). When we grew Ga_2O_3 on the p-type Si, the n-type Ga_2O_3 region, has higher electron concentration as majority carriers, and Si (p-type) has low electron concentration as minority carriers. This concentration gradient will enable the electrons to diffuse into the Si side, whereas the holes will diffuse into the Ga_2O_3 side. Thus, there will be depletion of electrons in

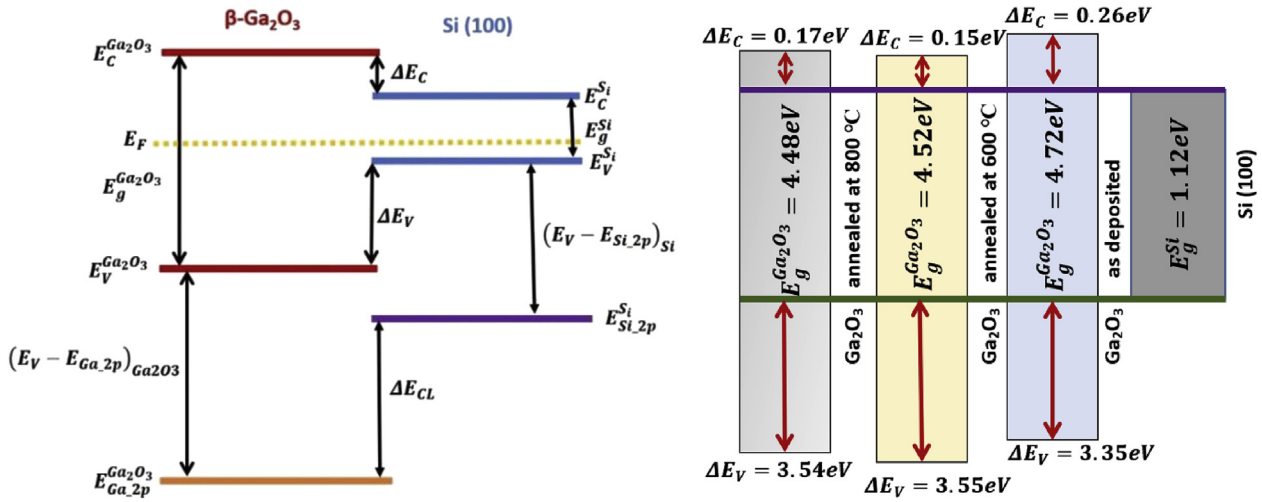

Fig. 6. (a) Schematic diagram of band alignment for Ga_2O_3/Si heterojunction. (b) Band offsets for all the Ga_2O_3 samples deposited on Si (100).

Table 4
Calculated parameters for band alignment of Ga_2O_3/Si heterojunction.

Parameters	As-deposited Ga_2O_3	Ga_2O_3 annealed at 600 °C	Ga_2O_3 annealed at 800 °C
ΔE_V	3.35 ± 0.05	3.55 ± 0.05	3.54 ± 0.05
ΔE_C	0.26 ± 0.02	0.15 ± 0.02	0.17 ± 0.02
$(E_V - E_{Si\_2p})_{Si}$	98.83 ± 0.1	98.83 ± 0.1	98.83 ± 0.1
$(E_V - E_{Ga\_2p})_{Ga2O3}$	1114.33 ± 0.1	1114.16 ± 0.1	1114.15 ± 0.1
ΔE_{CL}	1018.88 ± 0.1	1018.88 ± 0.1	1018.88 ± 0.1

Ga_2O_3 interface and will have depletion of holes in the Si interface [48]. From the Fermi level location, it can be said that the electron will be transferred from Ga_2O_3 to Si, and holes will tend to transfer from p-Si to Ga_2O_3 region. Furthermore, VBO of heterojunction is the barrier for the injection of holes, which will affect the efficiency of the Ga_2O_3/Si heterojunctions. Therefore, if the VBO value increases, the barrier for holes injection from Si to Ga_2O_3 will also increase.

Considering bandgap of as-deposited Ga_2O_3 thin film and Si to be 4.72 ± 0.05 eV and 1.12 ± 0.01 eV, respectively. The values of ΔE_V and ΔE_C have been calculated are to be 3.35 ± 0.05 eV and 0.26 ± 0.02 eV respectively. Thus, the conduction band level of Ga_2O_3 is above than that of Si, and the Valance band level of Ga_2O_3 is below the Si. Similar observations have been also noticed by Chen et al. [27] where VBO and CBO calculated for Ga_2O_3/Si (111) heterostructure are to be 3.5 and 0.2 eV respectively. We have also calculated the band offset values for Ga_2O_3 samples annealed at 600 °C and 800 °C that are listed in Table 4. VBO values of Ga_2O_3 thin film annealed at 600 °C and 800 °C are larger than as-deposited Ga_2O_3 samples. VBO is increased with higher annealing temperature because of possible diffusion of Si atoms from the substrate to the Ga_2O_3 film. The increase in the VBO can also be described by the development of a Ga silicate in the interfacial layer during the high annealing temperature [49]. It means if samples are annealed at a higher temperature, the efficiency of the devices will increase. However, if we compare both the annealed samples then the Ga_2O_3 sample annealed at 600 °C is better than annealed at 800 °C in respect of device efficiency because VBO value for the sample annealed at 600 °C is larger than sample annealed at 800 °C. There is a very minimal difference in the valance band offset (VBO) values of the sample annealed at 600 °C and 800 °C. This small difference in the VBO is due to the shift in the binding energy result is changes in the valance band maximum (VBM). From Table 3, the value of VBM for the sample annealed at 600 °C and 800 °C are 3.96 ± 0.1 and 4.032 ± 0.1 respectively. The core to core level binding energy for both the annealed samples is equal. Since VBM value of the sample annealed at 600 °C is smaller than the sample annealed at 800 °C, thus from the equation (2) VBO value will be higher for the sample annealed at 600 °C. We can conclude that among the three samples, the sample annealed at 600 °C could be best candidate for device purpose in term of efficiency. The comparison of band offsets for all the samples are shown in Fig. 6. (b) The parameters we obtained from present XPS study could be very essential to analyze the charge transfer mechanism of Ga_2O_3 based devices further.

4. Conclusion

In summary, Ga_2O_3 has been deposited on Si (100) substrate using PLD. The samples have been annealed at 600 °C and 800 °C under the vacuum environment. XRD data shows the polycrystalline nature of the thin films. The bandgap of Ga_2O_3 samples has been calculated using REELS technique. It shows a decrement with the increase in annealing temperature, whereas the work function is increasing with the increment in annealing temperature as determined using the UPS technique. In comparison with the annealed samples, the VBO of Ga_2O_3 thin film annealed at 600 °C is the largest due to possible interdiffusion of Si into Ga_2O_3. It is further concluded that the crystalline quality is degrading for both the higher and lower annealing temperature than the deposition temperature. Thereby, further annealing of the samples under vacuum environment can be avoided to preserve better crystallinity. However, on the contrary, the VBO is increasing with annealing temperatures. Therefore, annealing of the sample should improve the performance of the device applications involving band-offset related carrier transport assistance. Thus, a tradeoff between crystallinity and VBO needs to be maintained while annealing the Ga_2O_3/Si heterostructure for efficient and reliable device operations.

Declaration of competing interest

The authors declare that they have no known competing financial interests or personal relationships that could have appeared to influence the work reported in this paper.

Acknowledgments

The authors would like to acknowledge the Centre for Design and Fabrication of Electronic Devices (C4DFED) and Advanced Material Research Centre (AMRC), IIT Mandi, for the characterization facilities. We thank Mr. Priyamedha Sharma for his assistance with PLD and Mr. Naveen Kumar for XPS instrument. We would also like to acknowledge Science and Engineering Research Board (SERB), Govt. of India (ECR/2017/000810), for funding the project.

References

[1] T. Onuma, S. Saito, K. Sasaki, T. Masui, T. Yamaguchi, T. Honda, M. Higashiwaki, Valence band ordering in β-Ga2O3 studied by polarized transmittance and reflectance spectroscopy, Jpn. J. Appl. Phys. 54 (2015), https://doi.org/10.7567/JJAP.54.112601, 112601.
[2] M. Orita, H. Ohta, M. Hirano, H. Hosono, Deep-ultraviolet transparent conductive β-Ga 2 O 3 thin films, Appl. Phys. Lett. 77 (2000) 4166–4168, https://doi.org/10.1063/1.1330559.
[3] M.H. Wong, K. Sasaki, A. Kuramata, S. Yamakoshi, M. Higashiwaki, Field-plated Ga 2 O 3 MOSFETs with a breakdown voltage of over 750 V, IEEE Electron. Device Lett. 37 (2016) 212–215, https://doi.org/10.1109/LED.2015.2512279.
[4] Y. Yao, R. Gangireddy, J. Kim, K.K. Das, R.F. Davis, L.M. Porter, Electrical behavior of β-Ga2O3 Schottky diodes with different Schottky metals, J. Vac. Sci. Technol. B Nanotechnol. Microelect. Mater. Process. Meas. Phenom. 35 (2017), https://doi.org/10.1116/1.4980042, 03D113.
[5] M. Higashiwaki, H. Murakami, Y. Kumagai, A. Kuramata, Current status of Ga2O3 power devices, Jpn. J. Appl. Phys. 55 (2016), https://doi.org/10.7567/JJAP.55.1202A1, 1202A1.
[6] A.A. Dakhel, W.E. Alnaser, Experimental analysis of Ga2O3: Ti films grown on Si and glass substrates, Microelectron. Reliab. 53 (2013) 676–680, https://doi.org/10.1016/j.microrel.2013.01.010.
[7] K. Sasaki, M. Higashiwaki, A. Kuramata, T. Masui, S. Yamakoshi, Ga2O3 Schottky barrier diodes fabricated by using single-crystal β-Ga2O3 (010) substrates, IEEE Electron. Device Lett. 34 (2013) 493–495, https://doi.org/10.1109/LED.2013.2244057.
[8] K. Konishi, K. Goto, H. Murakami, Y. Kumagai, A. Kuramata, S. Yamakoshi, M. Higashiwaki, 1-kV vertical Ga2O3 field-plated Schottky barrier diodes, Appl. Phys. Lett. 110 (2017), https://doi.org/10.1063/1.4977857, 103506.
[9] S. Oh, J. Kim, F. Ren, S.J. Pearton, J. Kim, Quasi-two-dimensional β-gallium oxide solar-blind photodetectors with ultrahigh responsivity, J. Mater. Chem.

C 4 (2016) 9245–9250, https://doi.org/10.1039/C6TC02467J.
[10] A. Kumar, A. Bag, High responsivity of quasi-2D electrospun β-Ga2O3 based deep-UV photodetectors, IEEE Photonics Technol. Lett. 31 (2019), https://doi.org/10.1109/LPT.2019.2901236, 1–1.
[11] M. Ogita, K. Higo, Y. Nakanishi, Y. Hatanaka, Ga2O3 thin film for oxygen sensor at high temperature, Appl. Surf. Sci. 175 (2001) 721–725, https://doi.org/10.1016/S0169-4332(01)00080-0.
[12] M. Fleischer, H. Meixner, Sensing reducing gases at high temperatures using long-term stable Ga2O3 thin films, Sens. Actuators B Chem. 6 (1992) 257–261, https://doi.org/10.1016/0925-4005(92)80065-6.
[13] C. Baban, Y. Toyoda, M. Ogita, Oxygen sensing at high temperatures using Ga2O3 films, Thin Solid Films 484 (2005) 369–373, https://doi.org/10.1016/j.tsf.2005.03.001.
[14] S. Nakagomi, T. Momo, S. Takahashi, Y. Kokubun, Deep ultraviolet photodiodes based on β-Ga2O3/SiC heterojunction, Appl. Phys. Lett. 103 (2013), https://doi.org/10.1063/1.4818620, 72105.
[15] X.C. Guo, N.H. Hao, D.Y. Guo, Z.P. Wu, Y.H. An, X.L. Chu, L.H. Li, P.G. Li, M. Lei, W.H. Tang, β-Ga2O3/p-Si heterojunction solar-blind ultraviolet photodetector with enhanced photoelectric responsivity, J. Alloy. Comp. 660 (2016) 136–140, https://doi.org/10.1016/j.jallcom.2015.11.145.
[16] T. Oshima, T. Okuno, S. Fujita, Ga2O3 thin film growth on c-plane sapphire substrates by molecular beam epitaxy for deep-ultraviolet photodetectors, Jpn. J. Appl. Phys. 46 (2007) 7217, https://doi.org/10.1143/JJAP.46.7217.
[17] L.R. S.Z., Yonder Berencén1, Yufang Xie2, Wang3 Mao, Slawomir Prucnal4, Structural and Optical Properties of Pulsed-Laser Deposited Crystalline β-Ga2O3 Thin Films on Silicon, 2019, https://doi.org/10.1088/1361-6641/aafc90.
[18] P. Li, H. Shi, K. Chen, D. Guo, W. Cui, Y. Zhi, S. Wang, Z. Wu, Z. Chen, W. Tang, Construction of GaN/Ga 2 O 3 p–n junction for an extremely high responsivity self-powered UV photodetector, J. Mater. Chem. C. 5 (2017) 10562–10570, https://doi.org/10.1039/C7TC03746E.
[19] D. Guo, Y. Su, H. Shi, P. Li, N. Zhao, J. Ye, S. Wang, A. Liu, Z. Chen, C. Li, W. Tang, Deep ultra violet, ACS Nano 12 (2018) 12827–12835, https://doi.org/10.1021/acsnano.8b07997.
[20] D.Y. Guo, H.Z. Shi, Y.P. Qian, M. Lv, P.G. Li, Y.L. Su, Q. Liu, K. Chen, S.L. Wang, C. Cui, C.R. Li, W.H. Tang, Fabrication of β -Ga 2 O 3/ZnO heterojunction for solar-blind deep ultraviolet photodetection, Semicond. Sci. Technol. 32 (2017), https://doi.org/10.1088/1361-6641/aa59b0, 03LT01.
[21] C. He, D. Guo, K. Chen, S. Wang, J. Shen, N. Zhao, A. Liu, Y. Zheng, P. Li, Z. Wu, C. Li, F. Wu, W. Tang, α-Ga 2 O 3 nanorod array–Cu 2 O microsphere p–n junctions for self-powered spectrum-distinguishable photodetectors, ACS Appl. Nano Mater. 2 (2019) 4095–4103, https://doi.org/10.1021/acsanm.9b00527.
[22] P. Gollakota, A. Dhawan, P. Wellenius, L.M. Lunardi, J.F. Muth, Y.N. Saripalli, H.Y. Peng, H.O. Everitt, Optical characterization of Eu-doped β-Ga 2 O 3 thin films, Appl. Phys. Lett. 88 (2006), https://doi.org/10.1063/1.2208368, 221906.
[23] Z. Chen, X. Wang, F. Zhang, S. Noda, K. Saito, T. Tanaka, M. Nishio, M. Arita, Q. Guo, Observation of low voltage driven green emission from erbium doped Ga2O3 light-emitting devices, Appl. Phys. Lett. 109 (2016), https://doi.org/10.1063/1.4958838, 22107.
[24] M. Higashiwaki, K. Sasaki, A. Kuramata, T. Masui, S. Yamakoshi, Development of gallium oxide power devices, Phys. Status Solidi A 211 (2014) 21–26, https://doi.org/10.1002/pssa.201330197.
[25] J. Yang, S. Ahn, F. Ren, S.J. Pearton, S. Jang, A. Kuramata, High breakdown voltage (−201) $\beta $ -Ga2O3 Schottky rectifiers, IEEE Electron. Device Lett. 38 (2017) 906–909, https://doi.org/10.1109/LED.2017.2703609.
[26] A.J. Green, K.D. Chabak, M. Baldini, N. Moser, R. Gilbert, R.C. Fitch, G. Wagner, Z. Galazka, J. Mccandless, A. Crespo, Others, beta -Ga2O3 MOSFETs for Radio frequency operation, IEEE Electron. Device Lett. 38 (2017) 790–793, https://doi.org/10.1109/LED.2017.2694805.
[27] Z. Chen, K. Nishihagi, X. Wang, K. Saito, T. Tanaka, M. Nishio, M. Arita, Q. Guo, Band alignment of Ga2O3/Si heterojunction interface measured by X-ray photoelectron spectroscopy, Appl. Phys. Lett. 109 (2016), https://doi.org/10.1063/1.4962538, 102106.
[28] H. Peelaers, J.B. Varley, J.S. Speck, C.G. de Walle, Structural and electronic properties of Ga2O3-Al2O3 alloys, Appl. Phys. Lett. 112 (2018), https://doi.org/10.1063/1.5036991, 242101.
[29] C. Fares, F. Ren, E. Lambers, D.C. Hays, B.P. Gila, S.J. Pearton, Valence-and conduction-band offsets for atomic-layer-deposited Al 2 O 3 on (010)(Al 0.14 Ga 0.86) 2 O 3, J. Electron. Mater. 48 (2019) 1568–1573, https://doi.org/10.1007/s11664-018-06885-x.
[30] J.B. Varley, J.R. Weber, A. Janotti, C.G. de Walle, Oxygen vacancies and donor impurities in β-Ga 2 O 3, Appl. Phys. Lett. 97 (2010), https://doi.org/10.1063/1.3499306, 142106.
[31] A. Goyal, B.S. Yadav, O.P. Thakur, A.K. Kapoor, R. Muralidharan, Effect of annealing on β-Ga2O3 film grown by pulsed laser deposition technique, J. Alloy. Comp. 583 (2014) 214–219, https://doi.org/10.1016/j.jallcom.2013.08.115.
[32] Z. Feng, L. Huang, Q. Feng, X. Li, H. Zhang, W. Tang, J. Zhang, Y. Hao, Influence of annealing atmosphere on the performance of a β-Ga 2 O 3 thin film and photodetector, Opt. Mater. Express 8 (2018) 2229, https://doi.org/10.1364/OME.8.002229.
[33] Q. Cao, L. He, X. Feng, H. Xiao, J. Ma, Effect of annealing on the structural and optical properties of β-Ga2O3 films prepared on gadolinium gallium garnet (110) by MOCVD, Ceram. Int. 44 (2018) 830–835, https://doi.org/10.1016/j.ceramint.2017.10.006.
[34] D.Y. Guo, Z.P. Wu, Y.H. An, X.C. Guo, X.L. Chu, C.L. Sun, L.H. Li, P.G. Li, W.H. Tang, Oxygen vacancy tuned Ohmic-Schottky conversion for enhanced performance in β- Ga 2 O 3 solar-blind ultraviolet photodetectors, Appl. Phys. Lett. 105 (2014), https://doi.org/10.1063/1.4890524, 023507.
[35] K. Henkel, K. Karavaev, M. Torche, C. Schwiertz, Y. Burkov, D. Schmeißer, Al-oxynitride interfacial layer investigations for Pr X O Y on SiC and Si, J. Phys. Conf. Ser. 94 (2008), 012004, https://doi.org/10.1088/1742-6596/94/1/012004.
[36] M. Fleischer, W. Hanrieder, H. Meixner, Stability of semiconducting gallium oxide thin films, Thin Solid Films 190 (1990) 93–102, https://doi.org/10.1016/0040-6090(90)90132-W.
[37] G.A. Battiston, R. Gerbasi, M. Porchia, R. Bertoncello, F. Caccavale, Chemical vapour deposition and characterization of gallium oxide thin films, Thin Solid Films 279 (1996) 115–118, https://doi.org/10.1016/0040-6090(95)08161-5.
[38] Y. Liu, S.P. Singh, L.M. Kyaw, M.K. Bera, Y.J. Ngoo, H.R. Tan, S. Tripathy, G.Q. Lo, E.F. Chor, Mechanisms of ohmic contact formation and carrier transport of low temperature annealed Hf/Al/Ta on in 0.18 Al 0.82 N/GaN-on-Si, ECS J. Solid State Sci. Technol. 4 (2015) P30–P35, https://doi.org/10.1149/2.0111502jss.
[39] K. Kumar, G. Hughes, Synchrotron Radiation Based Photoemission Studies of Indium Oxide Passivation of ZnO (0001) Surface at High Temperature, 2018. ArXiv Preprint ArXiv:1810.00899. (Accessed 1 October 2018). arxiv:1810.00899v1 [cond-mat.mtrl-sci].
[40] C.-H. Ma, J.-H. Huang, H. Chen, Residual stress measurement in textured thin film by grazing-incidence X-ray diffraction, Thin Solid Films 418 (2002) 73–78, https://doi.org/10.1016/S0040-6090(02)00680-6.
[41] Y. Kokubun, K. Miura, F. Endo, S. Nakagomi, Sol-gel prepared β-Ga 2 O 3 thin films for ultraviolet photodetectors, Appl. Phys. Lett. 90 (2007), https://doi.org/10.1063/1.2432946, 31912.
[42] J.A. Chisholm, P.D. Bristowe, Formation energies of metal impurities in GaN, Comput. Mater. Sci. 22 (2001) 73–77, https://doi.org/10.1016/S0927-0256(01)00168-9.
[43] J.C. Carrano, T. Li, P.A. Grudowski, C.J. Eiting, R.D. Dupuis, J.C. Campbell, Current transport mechanisms in GaN-based metal–semiconductor–metal photodetectors, Appl. Phys. Lett. 72 (1998) 542–544, https://doi.org/10.1063/1.120752.
[44] N. Miura, T. Nanjo, M. Suita, T. Oishi, Y. Abe, T. Ozeki, H. Ishikawa, T. Egawa, T. Jimbo, Thermal annealing effects on Ni/Au based Schottky contacts on n-GaN and AlGaN/GaN with insertion of high work function metal, Solid State Electron. 48 (2004) 689–695, https://doi.org/10.1016/j.sse.2003.07.006.
[45] H. Kobayashi, H. Mori, T. Ishida, Y. Nakato, Zinc oxide/n -Si junction solar cells produced by spray-pyrolysis method, J. Appl. Phys. 77 (1995) 1301–1307, https://doi.org/10.1063/1.358932.
[46] H. Yang, Y. Qian, C. Zhang, D.-S. Wuu, D.N. Talwar, H.-H. Lin, J.-F. Lee, L. Wan, K. He, Z.C. Feng, Surface/structural characteristics and band alignments of thin Ga2O3 films grown on sapphire by pulse laser deposition, Appl. Surf. Sci. 479 (2019) 1246–1253, https://doi.org/10.1016/j.apsusc.2019.02.069.
[47] R. Puthenkovilakam, J.P. Chang, Valence band structure and band alignment at the ZrO 2/Si interface, Appl. Phys. Lett. 84 (2004) 1353–1355, https://doi.org/10.1063/1.1650547#.
[48] Z. Yuan, D. Li, M. Wang, P. Chen, D. Gong, P. Cheng, D. Yang, Electroluminescence of Sn O 2/p-Si heterojunction, Appl. Phys. Lett. 92 (2008), https://doi.org/10.1063/1.2902299, 121908.
[49] X. Fan, H. Liu, C. Fei, Effect of post-deposition annealing on the interfacial chemical bonding states and band alignment of atomic layer deposited neodymium oxide on silicon, Mater. Res. Express 1 (2014), https://doi.org/10.1088/2053-1591/1/4/045005, 045005.